Shahrood University of Technology

Journal of Hydraulic and Water Engineering (JHWE)

Journal homepage: https://jhwe.shahroodut.ac.ir/

Iranian Hydraulic Association (IHA)

Numerical Study of Effects of Inlet Geometry on Performance of Sediment Bypass Tunnels (SBTs) Using SSIIM Numerical Model

P. Aminian [1,*], M. Jorabloo [2] , A. Ahmadi [3]

[1*] Assistant Professor, Department of Civil Engineering, Shahrood Branch, Islamic Azad University, Shahrood, Iran.
[2] Assistant Professor, Department Water Engineering, Garmsar Branch, Islamic Azad University, Garmsar, Iran.
[3] Associate Professor, Department of Water and Environmental Engineering, Civil Engineering Collage, Shahrood University of Technology, Shahrood, Iran.

Article Info

Article history:
Received: 15 April 2023
Received in revised form: 28 May 2023
Accepted: 5 June 2023
Published online: 8 June 2023

DOI:
10.22044/JHWE.2023.13128.1020

Keywords
Deviated channel
Sediment bypass tunnels
Deviated flow
Secondary flow
SSIIM
Numerical model

Abstract

Sediment Bypass Tunnels (SBTs) are deviant channels that convey the current containing sediments from the upstream to the downstream of the reservoir. This study investigates the effect of hydraulic and geometry parameters such as discharge, flow depth, and deviated channel width on the deviating of the flow and sediment to the SBTs. In addition, the effects of the submerged plates with angels 30º, 45º, and 60º on the sediment transport to the 90-degree deviated channel (SBTs) were examined. The laboratory experiments were conducted in the flume with 10.0 m long, 0.60 m width, and 0.75 m height. Moreover, the SSIIM model was used to simulate flow and sediment. The results revealed that the 33% reduction of diversion channel width would lead to an 8.5% reduction of the deviated flow to the deviated channel. The maximum performance of deviated channel was obtained when the Froude number decreased and the flow depth increased. In terms of the angle of submerged plates, it can be observed that increasing the Froude number by 0.3 results in a 22.2% decrease in the channel deviated discharge and a 53.3% decrease in the channel deviated sediment. By reducing the Froude number of the flow and the depth along with using submerged plates at an angle of 30 degrees, the optimal diversion option can be provided. The comparison results of the numerical simulation of the SSIIM model with experiment data indicated that it simulated deviated flow and sediment to the SBTs with the correlation coefficient more than 0.95.

1. Introduction

Sediment transport in the river, especially when the eroded sediments enter the reservoirs, is one of the serious challenges in river engineering. Various topics in river engineering are of interest to the researchers; for example, we can mention the study of scouring downstream the of structures such as stilling basins (Hojjati and Zarrati, 2021; Hojjati et al., 2022), studying the sediment transport capacity of rivers (Jabary et al., 2014; Najafpour et al., 2016; Li and Wang, 2023), scouring around bridges (Wang et al., 2023), river mining management (Haghnazar and Saneie, 2019; Haghnazar et al., 2020), morphology of river (Zhang et al., 2023), etc. In order to control sedimentation in river and reservoirs, various methods can be used; for example, we can refer to the density current venting (Torabi Poudeh et al., 2014), flushing (Meshkati et al., 2009; Fathi-Moghadam et al.,

* *Corresponding author. E-mail address: p.aminian@gmail.com, Tel:+ 989121173188*

2010; Emamgholizadeh, 2012; Emamgholizadeh et al., 2013; Emamgholizadeh and Fathi Moghadam, 2014), Sediment Bypass Tunnels (SBTs) (Aminian et al., 2019a; Aminian et al., 2019b; Koshiba et al., 2022), etc. SBTs are deviant channels that convey the current containing sediments from the upstream to the downstream of the reservoir and in addition, they used to maintain long-term useful reservoir volume along with increasing the efficiency of hydroelectricity production. Proper management of SBTs would safely remotely manage the sediment accumulation away from power plant intakes in addition to having a positive impact on ecology because sediment transport may reduce corrosion in the riverbed or even stop it (Morris and Fan, 1997). According to Auel and Boes (2011), there are generally two different SBT types: type A inlet flow with free surface conditions in the Delta and type B, which usually operates under pressure, under sediments. These deviant tunnels must have enough slope to prevent sedimentation but should be as gentle as possible to prevent erosion by limiting the flow rate. The first SBTs were constructed in Japan, and then Switzerland in the early 20th century, and a decade was dedicated to reducing their construction rates (Vischer, 1997; Sumi et al., 2004). The SBT of Nunabiki Dam was the first SBT in Japan, which was built in 1908, eight years after the construction of dam in 1900. This tunnel is estimated to work at the reservoir for 25 to 1000 years. The SBT type A is another example of the Asahi Dam in Japan that has greatly reduced the volume of sediment formed after its launch in 1998, and even during a major flood in 2011, the sediment path around the dam helped to limit the internal flow of sediments inside the reservoir (Boes et al., 2014). Kondolf et al. (2014) presented a general equilibrium of the reduction of life of the world's dams reservoirs due to trapping sediments that inevitably diminishes human ability to supply the water and electricity needed for population growth. Recent research on the SBT subject has focused on tunnels resistance to hydraulic erosion as well as combining laboratory res earch and numerical models (Kantoush et al., 2011; Boes et al., 2014), where they have investigated the flow properties and concentration of Suspended Sediment Flows (SSCs) in a model with a scale from its actual sample (seasonal flood diversion of SBTs). Jenzer Althaus et al. (2014) designed a main system for delivering flushing suspended materials to facilitate flushing operation (Jenzer Althaus et al., 2014).

Emamgholizadeh and Samadi (2008) and Emamgholizadeh (2018) conducted a study on the using of the SBT method at the upstream of the Dez Reservoir Dam, and concluded that construction of a submerged dam at a distance of 9 km from the dam as well as building a tunnel with a diameter of 28.8 m and a length 15 km could improve the possibility to discharge 11.3 million cubic meters of sediment. The Salis Dam reservoir is another example that lost half of its reservoir volume in 26 years (1986-2012). Approximately 80,000 cubic meters of sediments from the Albula River had entered the reservoir prior to construction of the SBT; however, after the SBT was built, the volume of the sediment entering the reservoir was significantly reduced. Various factors can affect the flow deviation as well as the rate of sediment transport within the Sediment Bypass Tunnel. When the river water flow reaches the SBT, part of the flow diverts to the SBT in proportion of the channel's absorption intensity. This flow deviation causes changes in the hydraulic conditions of the river. Examination of the velocity profile shows that the secondary flow is similar to that found in the curvature of the river. The higher the ratio of the inlet flow to the flow rate in the main channel, the higher the produced secondary flow. Therefore, any action taken to increase the eddy currents and secondary flows in the SBT inlets will increase the sediment input to the secondary channel (Neary, 1992). The flow in the SBT inlet, the complexity of the sediment transport phenomenon, the influence of increasing sediment input, and the increase in sediment

transport capacity of the main channel on the bed morphology have led to further research in this area (Neary et al., 1999). According to studies, the three-dimensional flow pattern to the secondary channel is similar to Fig. 1 (Neary et al., 1999).

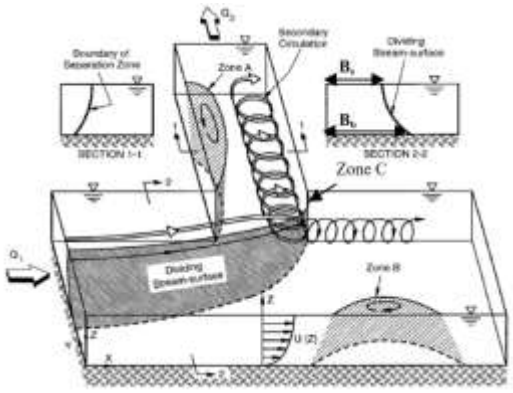

Figure 1. Inlet flow pattern of the secondary channel (deviated channel) (Neary et al., 1999).

Previous studies show that many researchers used vane structure at the water intake to control passing sediment (Emamgholizadeh and Torabi, 2008; Al-Zubaidy and Ismaeil, 2022; Taşar et al., 2023) or control scouring around the bridge abutment (Nohani, 2017; Chauhan et al., 2023).

In addition to experimental study, also other researchers used different numerical models to simulate sediment transport to water intake (Neary et al., 1999). In this study, the SSIIM model was used to study of the influence of inlet geometry on the performance of the sediment bypass tunnel. This model was used successfully in previous studies of sediment transport (Ruether et al., 2005; Hamidi and Siadatmousavi, 2017; Lai and Wu, 2018). For example, Ruether et al. (2005) applied SSIIM model to compute sediment transport at water intakes. Their results showed that SSIIM model performed well to compute the sediment concentrations which entered to the water intake. Lai and Wu (2018) studied sediment bypass tunnels at Shihmen reservoir in Taiwan by numerical model. They used physical model data to test model performance, and finally proposed sediment bypass plans.

Literature review indicates that no research has been conducted so far to investigate the effect of inlet geometry of SBTs on its performance in flow and sediment deviation. For this purpose, the effect of hydraulic and geometrical factors of SBTs on the deviated flow and sediments has been investigated using experimental studies and appropriate alternatives for transfer and deviation of the maximum sediments with the least amount of flow were suggested. Experiments were also conducted in two cases: without submerged plates and with submerged plates, and the results were compared with each other, and the impact of using submerged plates on flow and sediment deviation was investigated. Finally, flow and sediment simulations were performed using SSIIM numerical model, and compared with laboratory results.

2. Materials and Methods

2.1. Theory

The main variables that affect the performance of the SBTs channel is the main channel width (B), the secondary channel width (b), the longitudinal slope of the main channel (S_0), the submerged plate angle (Θ), the average speed of flow in the main channel (U), the flow depth in the main channel (y), the flow rate in the main channel (Q_m), the flow rate in the secondary channel (Q_l), the deviated flow ratio (Q_r), sedimentation flow in the main channel(Q_{sm}), sedimentation flow in the secondary channel (Q_{sl}), the deviated sub-dimension flow ratio(Q_s), average material diameter (d_{50}), sediment specific weight (ρ_s), the standard deviation of the distribution of aggregate size (σ_g), water specific weight (ρ), gravitational acceleration (g), and fluid kinematic viscosity (ν).

By defining the parameters $Q_r = {}^{Q_l}/_{Q_m}$ and $Q_s = {}^{Q_{sl}}/_{Q_{sm}}$ Equation (1) is obtained:

$$f(Q_r, Q_s, U, S0, b, y, B, \Theta, d_{50}, \sigma g, \nu, \rho, \rho s, g) = 0 \quad (1)$$

Using the Buckingham-π theorem and removing the constant parameters, the following dimensionless equation is achieved:

$$Q_s = f\left(\frac{y}{B}, \frac{b}{B}, Fr, \Theta\right) \quad (2)$$

2.2. Experimental procedure

The laboratory flume used in this study is a sloping straight rectangular section 10 meters long, 0.6 meters wide, and 0.75 meters high. The bed material was made of painted metal plate, and the walls were made of glass with 8 mm thickness (Fig. 2). The location of the secondary channel, which is a rectangular channel with a length of 2.2 m, is at a distance of 4 m from the beginning of the flume.

Figure 2. A view of the main and secondary channels.

In order to investigate sediment transport to the secondary channel, silica sand with uniform grading (with a mean diameter of 1.1 mm and a uniformity coefficient of 1.41) was used. The granulation curve is shown in Fig. 3. The duration of the tests dependent to the flow conditions, for low discharges it was about 2 hours, and for high discharge it was about 30 minutes.

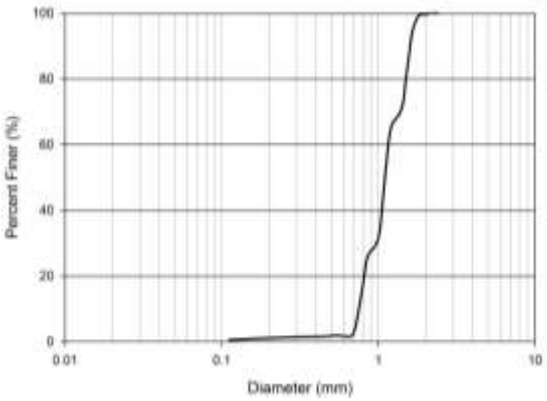

Figure 3. Grain-size distribution curve of sediment.

Prior doing each experiment, the bed sediment with uniform grading (D_{50} = ,1.1 mm and $\sigma_g = 1.41$) was placed as a 5 cm thick layer along the whole length of the flume. At the end of each experiment, the scoured sediments were then collected at the end of the main channel and secondary channel and drained in specially screened sieves, and after being placed in the oven, the weight of the sediments was measured (Fig. 4). Three submerged plates with 7 mm height were used. Submerged plates were arranged at one-third the width of the main channel, and were attached to the wall opposite the secondary channel (Fig. 5). The experiments were carried out in three angles of submerged plates 30, 45, and 60 degrees relative to the axis of flow, with constant holding of 50, 70, and 98 mm depth for each of 5 different discharges, which led to 5 different Froude numbers, and the results were compared with the condition without using submerged plates. Table 1 demonstrates the values of the variables in the experiments and the number of experiments performed. According to Table 1, 60 tests were performed to compare different situations.

Figure 4. Leaching of sediments in the main channel.

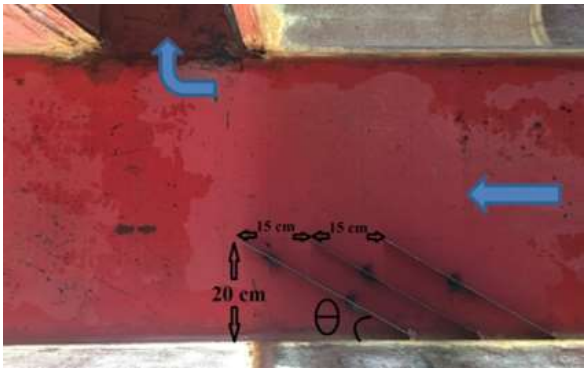

Figure 5. Dimensions of submerged plates in the main channel.

Table 1. Values of variables for tests without submerged plates and submerged plates with angles 30, 45, and 60 degrees.

Test No.	Flow Depth (cm)	Main channel discharge (L/s)	Froude number
1	50	13.5	0.64
2	50	15.25	0.73
3	50	17	0.81
4	50	18.5	0.88
5	50	20	0.95
6	70	23	0.66
7	70	25.5	0.73
8	70	28	0.80
9	70	30.5	0.88
10	70	33	0.95
11	98	38	0.66
12	98	42	0.73
13	98	46	0.80
14	98	51	0.88
15	98	56	0.97

2.3. SSIIM numerical model

This model has been developed to hire in hydraulic and sediment engineering. The basis of this model is the Finite Volume Method (FVM), which has a non-orthogonal network with three-dimensional organization. For the hydraulic flow section, this model solves the Navier-Stokes equations for the turbulent flow in three directions and solves the convection-diffusion equation for sediment transport. The Navier-Stokes equations incorporated in the SSIIM model for constant and non-compressible density currents are (Olsen, 2006):

$$\frac{\partial U_i}{\partial t} + U_j \frac{\partial U_i}{\partial x_j} = \frac{1}{\rho} \frac{\partial}{\rho \partial x_j} (-P\delta_{ij} - \overline{\rho u_i u_j}) \qquad (3)$$

in which U is the flow velocity, P is the pressure, and δ_{ij} is Kronecker delta (if i = j, its value is 1 and its value is zero if i ≠ j). Also in the above equation, the first and second expressions on the left side are transient term and transfer term, respectively. On the right side of the above equation, the first and second terms are Reynolds stress term and stress term, respectively. The above equations are discretized by the control volume method, and the non-explicit method is used to solve them. In the above equation, the SIMPLE method is used to correct the pressure. The Reynolds stresses model, using Boussinesq's idea, is required to solve the above equation. The Boussinesq equation is:

$$\frac{\partial U_i}{\partial t} + U_j \frac{\partial U_i}{\partial x_j} = \frac{1}{\rho} \frac{\partial}{\rho \partial x_j} (-P\delta_{ij} - \overline{\rho u_i u_j}) \qquad (4)$$

By placing the Boussinesq equation in the Navier-Stokes equation, it can be written as follows:

$$\frac{\partial U_i}{\partial t} + U_j \frac{\partial U_i}{\partial x_j} = \frac{1}{\rho} \frac{\partial}{\partial x_j} \left[-\left(p + \frac{2}{3} k \right) \delta_{ij} + \right.$$
$$\left. + \nu_T \frac{\partial U_i}{\partial x_j} + \nu_T \frac{\partial U_i}{\partial x_i} \right] \qquad (5)$$

The kinematic viscosity (υ_T) in the above equation results from the turbulence. Moreover, the K-epsilon (k-ε) turbulence model has been hired to calculate ν_t, where the

ν_t equation and K-epsilon (k-ε) turbulence model could be written as follows:

$$\nu_t = C_\mu \frac{k^2}{\varepsilon} \quad (6)$$

in which C_μ is the constant coefficient, υ_T is the eddy viscosity, k is the kinetic energy, and ε is the dissipation. The above two-dimensional equations are solved separately for $k(\{x_i\},t)$ and $\varepsilon(\{x_i\},t)$, until the eddy viscosity value of $\nu_t(\{x_i\},t)$ is obtained. In the K-epsilon (k-ε) turbulence model, the transient equations are modeled as follows (Olsen, 2005):

k – transport

$$\frac{\partial k}{\partial t} + U_i \frac{\partial k}{\partial x_i} = \frac{\partial}{\partial x_i}\left(\frac{\nu_t}{\sigma_k}\frac{\partial k}{\partial x_i}\right) + \nu_t\left(\frac{\partial U_i}{\partial x_j} + \frac{\partial U_i}{\partial x_i}\right)\frac{\partial U_i}{\partial x_j} - \varepsilon$$

ε – equation

$$\frac{\partial \varepsilon}{\partial t} + U_i \frac{\partial \varepsilon}{\partial x_i} = \frac{\partial}{\partial x_i}\left(\frac{\nu_t}{\sigma_k}\frac{\partial \varepsilon}{\partial x_i}\right) + C_{1\varepsilon}\frac{\varepsilon}{k}\nu_t\left(\frac{\partial U_i}{\partial x_j} + \frac{\partial U_i}{\partial x_i}\right)\frac{\partial U_i}{\partial x_j} - C_{2\varepsilon}\frac{\varepsilon^2}{k}$$

in which $C_{\varepsilon 1}$ and $C_{\varepsilon 2}$ are constant values. In the equations, k and ε, the left-hand terms, which include the local or transition time terms and the horizontal displacement term are balanced with the right-hand terms, which include the spread, production and loss terms or turbulence disappearance terms. The K-epsilon (k-ε) turbulence model is usually used with 5 constant coefficients, where the standard values of the constant coefficients in the K-epsilon (k-ε) turbulence model are given in Table 3 (Abbott and Minns, 2017):

Table 3. Standard values of the constant coefficients in the K-epsilon (k-ε) turbulence model (Abbott and Basco, 1997).

c_μ	$C_{1\varepsilon}$	$C_{2\varepsilon}$	σ_K	σ_ε
0.09	1.44	1.92	1.01	1.30

σ_ε and σ_K are known as the turbulent Prandtl number (Pr_t). So far, the K-epsilon (k-ε) turbulence model has been used successfully to simulate real, two- or three-dimensional flows. Experience has shown, however, that the K-epsilon (k-ε) turbulence model equations are very sensitive to $C_{\varepsilon 1}$ and $C_{\varepsilon 2}$ constant values. The C_μ coefficient value depends on the local non-uniform properties of some turbulent flows.

In the SSIIM model, the suspended charge (c) is calculated using the convection-diffusion equation:

$$\frac{\partial c}{\partial t} + U_j \frac{\partial c}{\partial x_j} + w\frac{\partial c}{\partial z} = \frac{\partial c}{\partial x_j}\left(\Gamma_\Gamma \frac{\partial c}{\partial x_j}\right) \quad (9)$$

In the above equation, c is the sediment concentration, ω is the particle deposition rate, U is the flow rate, x is the distance dimension, and Γ is the diffusion coefficient. The diffusion coefficient (Γ_Γ) has been taken from the K-epsilon (k-ε) turbulence model:

$$\Gamma_\Gamma = \frac{\nu_\Gamma}{S_C} \quad (10)$$

In which S_c is the Schmidt number that is set to 1 by default.

Van Rijn obtained the following formula to calculate the bed load (q_b) that is used as the program default in the SSIIM model:

$$\frac{q_b}{D_{50}^{1.5}\sqrt{\frac{(\rho_s-\rho)g}{\rho}}} = 0.053\frac{\left[\frac{\tau-\tau_c}{\tau_c}\right]^{1.5}}{D_{50}^{0.3}\left[\left(\frac{(\rho_s-\rho)g}{\rho\nu^2}\right)\right]^{0.1}} \quad (11)$$

3. Results and Discussion

Based on the experimental results, the effects four non-dimensional parameters namely, $\frac{B}{y}, \frac{B}{y}$, Fr, and θ were invesitigated on the $Q_s = Q_{sl}/Q_{sm}$ as follows:

3.1. Effect of B/y on ratio of deviated sediments to total sediments (Q_s)

Figures (6) to (8) indicate the effect B/y on the Q_s for a constant flow depth. As shown in these figures, the amount of deviated sediment

increases with an increase in the width of the deviated channel for different Froude numbers. A quantitative analysis of the results shows that the increase Froude number results in an average 44% decrease in the amount of sediments diverted to the secondary channel. By changing the width of the deviated channel by 1.5 times of its original size, the deviated sedimentation rate for $\frac{y}{B}$ = 0.08, $\frac{y}{B}$ = 0.12, and $\frac{y}{B}$ = 0.16 would increase by 20.3%, 9.37%, and 9.68%, respectively. An increase of 1.5 times the width of the deviated channel can be effective in increasing the deviated sediment to the secondary channel by 13%. According to the results, it can be concluded that increasing the width of the secondary channel can be effective in increasing the deviated sediments to the secondary channel.

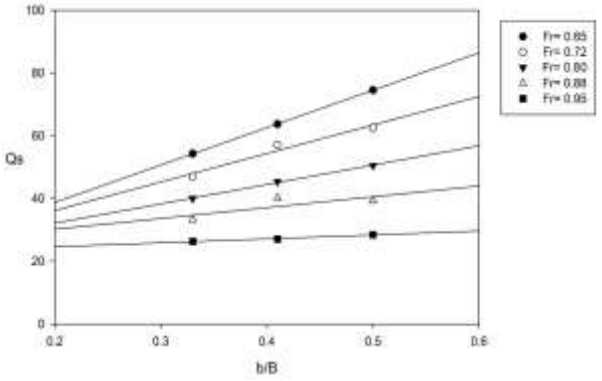

Figure 6. Changes of the ratio of deviated sediments to total sediments (Q_s) with b/B for $\frac{y}{B}$ = 0.08.

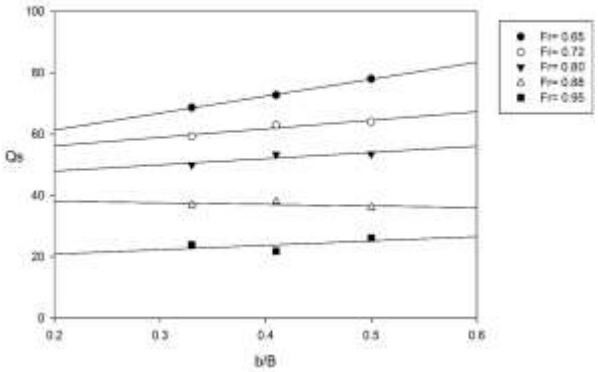

Figure 7. Changes of the ratio of deviated sediments to total sediments with b/B for $\frac{y}{B}$ = 0.12.

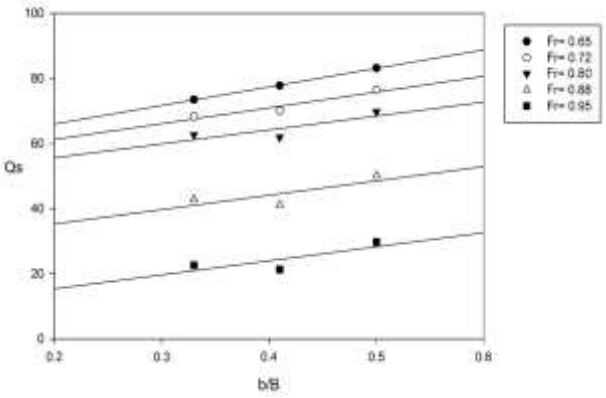

Figure 8. Changes of the ratio of deviated sediments to total sediments with b/B for $\frac{y}{B}$ =0.16.

3.2. Effect of angle of submerged plates (Θ) on Q_s

Figures 9 to 11 show the effect of the angle of submerged plates on the amount of deviated sediments at different depths. It is evident that by increasing the plate angles at a ratio of $\frac{y}{B}$ = 0.08, the amount of deviated sediment decreases but with increasing the depth of flow to $\frac{y}{B}$ = 0.16, no change in the amount of deviated sediment was observed, such that by increasing the plate angles twice their original value, the deviated sedimentation rate was reduced to 18.3% for y/B = 0.08, 9% for y/B = 0.12, and 2.1% for y / B = 0.16. By applying submerged plates at 60-degree angle, the sediment deviation compared to the no submerged plates condition was decreased by 12.4% for y / B = 0.08 and 3.4% for y / B = 0.12 but increased by 4.4% for y / B = 0.16. The use of 60° angles is only effective for high depths and to a small extent, and the 30° angle has better results in sediment transport.

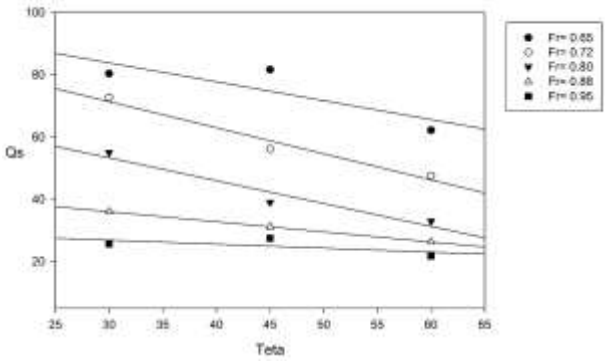

Figure 9. Changes of the ratio of deviated sediments to total sediments with Θ at $\frac{y}{B}$ = 0.08.

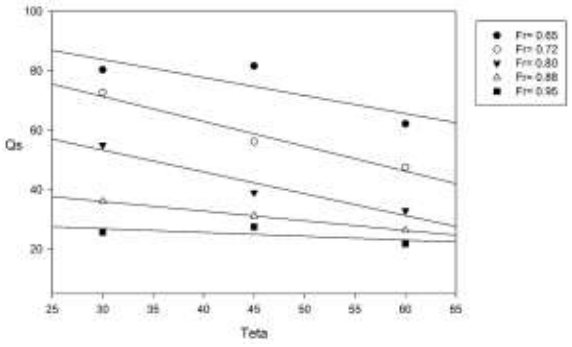

Figure 10. Changes of the ratio of deviated sediments to total sediments with Θ at $\frac{y}{B}$ = 0.12.

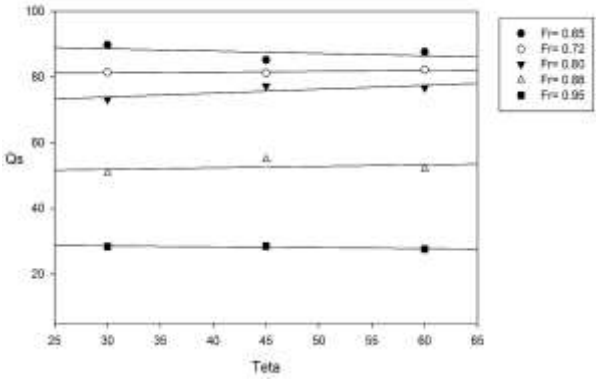

Figure 11. Changes of the ratio of deviated sediments to total sediments with Θ at $\frac{y}{B}$ = 0.16.

According to the results, it can be concluded that the 90-degree deviated channel has a good performance in sediment transport. The results showed that the use of submerged plates will increase the amount of deviated sediment compared to the deviated flow discharge to the SBT but the angle variations do not have a significant effect on this amount because the plate length decreases with an increase in plate angles and the interaction between the flow and the centrifugal force is reduced and smaller amounts of discharge enter the secondary channel.

3.3. Result from SSIIM model

In order to calibrate the SSIIM model, it is necessary to have the required experimental or field data where in this research, the experimental data was used. Evaluation of the model was conducted by comparing the volume of passing sediments and measured sediments. Since the mathematical model can only compute the conditions presented to the model in an algebraic manner and cannot physically understand the phenomenon, it is not enough to simply design and use a mathematical model to answer it. Therefore, it is necessary to analyze the results and figures calculated and compare them with reality. For this purpose, the results of water level profile were used. To calibrate the model, five roughness coefficients $ks = 0.0020\ m$, $ks = ds = 0.0012\ m$, $ks = 0.0030\ m$, $ks = 2ds = 0.0024\ m$, $ks = 3ds = 0.0036\ m$ were introduced to the model. The comparison showed that in the case of roughness coefficient $ks = 2ds$, the water surface profile calculated by the model is in good agreement with the measured water surface profile. Examination of flow velocity vectors and similar velocity lines after the model was calibrated indicated that the velocity vectors maintained their extended state approximately 2m from the beginning of the channel inlet and approaching the secondary channel caused the velocity vectors to lose their extended state current. After calibrating the hydrodynamic model, the SSIIM model used to predict the volume of transmitted sediments at the main channel and deviated channel. The SSIIM model uses different sediment transport equations namely, Van Rijn, England-Hansen, Ackers-White, Yang, Shen-Hang and Einstein to calculate sediment transport. Table 2 indicates the results of SSIIM model implementation to calculate the relative of

deviated sediments to the total sediments ($Q_s = Q_{sl} / Q_{sm}$) and compared with those of measured values.

Table 2. Comparison between measured and calculated of deviated sediments to the SBTs.

Sediment transport formula	(Yang)	(Van Rijn)	(Einstein)	(Shen/Hung)	(Ackers/ White)
calculated $Q_s = Q_{sl} / Q_{sm}$ by the SSIIM model	-	54.9 %	48.2%	12.7%	11.4%
measured $Q_s = Q_{sl} / Q_{sm}$ in laboratory	67%	67%	67%	67%	67%
Error (%)	-	18%	28%	81%	83%

A comparison between the calculated of deviated sediments to the SBTs by the SSIIM model and measured values indicated that the Van Rijn formula, with 18 % error, was able to calculate the percentage of deviated sediments to total sediments better than the other formulas. Also the implementation of the model using Yang current formula had a problem and could not calculate the percentage of deviated sediments to total sediments.

4. Conclusion

The laboratory results regarding the width of the deviated channel highlight the following results:

- Increasing the Froude number on average results in a 44% decrease in the sediments diverted to the secondary channel.
- An increase of 1.5 times the width of the deviated channel can be effective in increasing the deviated sediment to the secondary channel by 13%.
- Reducing the Froude number and increasing the width of the deviated channel can be effective in increasing the deviation of sediments to the secondary channel.
- By doubling the angle of the plates, the amount of deviated sediment is reduced by an average of 9.8%.
- By applying submerged plates at an angle of 60°, the amount of deviated sediments increases on average by 6.7% compared to the condition with no submerged plates.
- Plates with a 60-degree angle are only effective for high depths and to a very low degree, and a 30-degree angle gives better results in sediment transport.
- The use of submerged plates will increase the amount of deviated sediments relative to the deviated flow discharge to the SBT but the angle changes will not have a significant effect on this value.
- The results of the SSIIM numerical modeling highlight that the Van Rijn formula, with 18% error, was able to calculate the percentage of deviated sediments to total sediments better than the other formulas.

Data Availability

The data used to support the findings of this study is available from the corresponding author upon request.

Conflicts of Interest

The authors declare that they have no conflicts of interest regarding the publication of this paper.

References

Abbott, M.B., and Minns, A.W., 2017. Computational hydraulics. Routledge.

Al-Zubaidy, R.A., and Ismaeil, R.H., 2022. Sediment control at the lateral channel inlet, IOP Conference Series: Earth and Environmental Science. IOP Publishing, pp. 012096.

Aminian, P., Ahmadi, A., and Emamgholizadeh, S., 2019a. Experimental investigation on the deviated sediment and flow to sediment bypass tunnels (SBTs) using submerged plates. *Journal of Hydraulic Structures*, 5(2), pp. 18-31.

Aminian, P., Ahmadi, A., and Emamgholizadeh, S., 2019b. Experimental Study of the Effects of Hydraulic and Geometric Parameters of the Sediment Transport Tunnel on the Deviation Flow and Transmitted Sediment. *Iranian*

Journal of Soil and Water Research, 50(2), pp. 505-514.

Auel, C., and Boes, R.M., 2011. Sediment bypass tunnel design–review and outlook. *Dams and reservoirs under changing challenges*, 40312.

Boes, R., Auel, C., Hagmann, M., and Albayrak, I., 2014. Sediment bypass tunnels to mitigate reservoir sedimentation and restore sediment continuity. *Reservoir sedimentation*, pp. 221-228.

Chauhan, V., Padhi, E., Chavan, R., and Singhal, G.D., 2023. A review of bridge scour mitigation measures using flow deflecting structures. *ISH Journal of Hydraulic Engineering*, pp. 1-14.

Emamgholizadeh, S., 2012. Neural network modeling of scour cone geometry around outlet in the pressure flushing. *Global NEST Journal*, 14(4), pp. 540-549.

Emamgholizadeh, S., Bateni, S.M., and Jeng, D.-S., 2013. Artificial intelligence-based estimation of flushing half-cone geometry. *Engineering Applications of Artificial Intelligence*, 26(10), pp. 2551-2558.

Emamgholizadeh, S., and Fathi Moghadam, M., 2014. Pressure Flushing of Cohesive Sediment in Dam Reservoir. *Journal of Hydrology*, 19(1), pp. 674-681.

Emamgholizadeh, S., and Samadi, H., 2008. Desilting of deposited sediment at the upstream of the Dez reservoir in Iran. *Journal of Applied Sciences in Environmental Sanitation*, 3(1), pp. 25-35.

Emamgholizadeh, S., and Torabi, H., 2008. Experimental investigation of the effects of submerged vanes for sediment diversion in the Veis (Ahwaz) Pump Station. *Journal of Applied Sciences*, 8(13), pp. 2396-2403.

Fathi-Moghadam, M., Emamgholizadeh, S., Bina, M., and Ghomeshi, M., 2010. Physical modelling of pressure flushing for desilting of non-cohesive sediment. *Journal of Hydraulic Research*, 48(4), pp. 509-514.

Haghnazar, H., and Saneie, M., 2019. Impacts of pit distance and location on river sand mining management. *Modeling Earth Systems and Environment*, 5, pp. 1463-1472.

Haghnazar, H., Sangsefidi, Y., Mehraein, M., and Tavakol-Davani, H., 2020. Evaluation of infilling and replenishment of river sand mining pits. *Environmental Earth Sciences*, 79, pp. 1-18.

Hamidi, A., and Siadatmousavi, S.M., 2017. Numerical simulation of scour and flow field for different arrangements of two piers using SSIIM model. *Ain Shams Engineering Journal*.

Hojjati, S.H., and Zarrati, A.R., 2021. Numerical study of scouring downstream of a stilling basin. *Environmental Fluid Mechanics*, 21, pp. 465-482.

Hojjati, S.H., Zarrati, A.R., and Dehnavi, M.N., 2022. Experimental study of scouring downstream of USBR Type I stilling basin aligned with or below the erodible bed. *Sādhanā*, 47(4), pp. 272.

Jabary, A., Hosseini, A., Haghiabi, A.H., Emamgholizadeh, S., and Behnia, A., 2014. Prediction of the sediment load in the river by HEC-RAS. *Irrigation and Water Engineering*, 4(4), pp. 12-23.

Jenzer Althaus, J.M., Cesare, G.D., and Schleiss, A.J., 2014. Sediment evacuation from reservoirs through intakes by jet-induced flow. *Journal of Hydraulic Engineering*, 141(2), pp. 04014078.

Kantoush, S., Sumi, T., and Murasaki, M., 2011. Evaluation of sediment bypass efficiency by flow field and sediment concentration monitoring techniques. *Journal of Japan Society of Civil Engineers, Ser. B1 (Hydraulic Engineering)*, 67(4), pp. I_169-I_174.

Kondolf, G.M. et al., 2014. Sustainable sediment management in reservoirs and regulated rivers: Experiences from five continents. *Earth's Future*, 2(5), pp. 256-280.

Koshiba, T., Miura, S., and Sumi, T., 2022. Study on the Koshibu Dam sediment bypass tunnel operation based on sediment transport monitoring in upstream reaches, E3S Web of Conferences. EDP Sciences, pp. 03013.

Lai, Y.G., and Wu, K.-w., 2018. A numerical modeling study of sediment bypass tunnels at shihmen reservoir, Taiwan. *International Journal of Hydrology*, 2, pp. 72-81.

Li, B., and Wang, Y., 2023. Dynamics of sediment transport in the Yangtze River and their key drivers. *Science of The Total Environment*, 862, pp. 160688.

Meshkati, M., Dehghani, A., Naser, G., Emamgholizadeh, S., and Mosaedi, A., 2009. Evolution of developing flushing cone during the pressurized flushing in reservoir storage.

World Academy of Science, Engineering and Technology, 58, pp. 1107-1111.

Morris, G., and Fan, J., 1997. Chapter 9. Hydraulics of Sediment Transport, in "Reservoir Sedimentation Handbook-Design and Management of Dams, Reservoirs, and Watersheds for Sustainable Use". McGraw Hill, New York.

Najafpour, N., Emamgholizadeh, S., Torabi Podeh, H., and Haghiabi, A.H., 2016. Estimation of Sediment Transport Rate of Karun River (Iran). *Journal of Hydraulic Structures*, 2(2), pp. 74-84.

Neary, V., Sotiropoulos, F., and Odgaard, A., 1999. Three-dimensional numerical model of lateral-intake inflows. *Journal of Hydraulic Engineering*, 125(2), pp. 126-140.

Neary, V.S., 1992. Flow structure at an open channel diversion, University of Iowa.

Nohani, E., 2017. Application of the Submerged Vanes on Reduction of Local Scour around the Bridge Abutment with Rounded Nose. *Irrigation and Drainage Structures Engineering Research*, 18(68), pp. 113-128.

Olsen, N.R., 2006. A three-dimensional numerical model for simulation of sediment movements in water intakes with multiblock option. Department of Hydraulic Environmental Engineering, Norwegian University of Science Technology, Trondheim, Norway.

Ruether, N., Singh, J., Olsen, N., and Atkinson, E., 2005. 3-D computation of sediment transport at water intakes, Proceedings of the Institution of Civil Engineers-Water Management. Thomas Telford Ltd, pp. 1-7.

Sumi, T., Okano, M., and Takata, Y., 2004. Reservoir sedimentation management with bypass tunnels in Japan, Proc. 9th International Symposium on River Sedimentation, pp. 1036-1043.

Taşar, B., Üneş, F., Gemici, E., Demirci, M., and Kaya, Y.Z., 2023. NUMERICAL MODELING OF SUBMERGED VANE FLOW. *Aerul si Apa. Componente ale Mediului*, pp. 111-120.

Torabi Poudeh, H.T., Emamgholizadeh, S., and Fathi-Moghadam, M., 2014. Experimental study of the velocity of density currents in convergent and divergent channels. *International Journal of Sediment Research*, 29(4), pp. 518-523.

Vischer, D., 1997. Bypass tunnels to prevent reservoir sedimentation, Proc. 19th ICOLD Congress, Florence, Italy, 1997.

Wang, T., Reiffsteck, P., Chevalier, C., Zhu, Z., Chen, C.-W., and Schmidt, F., 2023. A novel extreme gradient boosting algorithm based model for predicting the scour risk around bridge piers: application to French railway bridges. *European Journal of Environmental and Civil Engineering*, 27(3), pp. 1104-1122.

Zhang, H. et al., 2023. Morphology and origin of liquefaction-related sediment failures on the Yellow River subaqueous delta. *Marine and Petroleum Geology*, 153, pp. 106262.